

# BOX BEHNKEN DESIGN METHOD TO OPTIMISE PIEZOELECTRIC CANTILEVER-BASED ENERGY HARVESTING SYSTEM PARAMETERS FOR EFFICIENT EXPERIMENTATION

Sunday Ayoola Oke<sup>1\*</sup>, Ibraheem Adedotun Abdul<sup>2</sup>, Ismaila Badmus<sup>2</sup>, Oluwatomiwa Akinola<sup>1</sup>, John Rajan<sup>3</sup>, Swaminathan Jose<sup>4</sup>, Adekunle Adetayo Yekinni<sup>5</sup>, Kabiru Alani Olaiya<sup>5</sup>

<sup>1</sup>Department of Mechanical Engineering, University of Lagos, Lagos, Nigeria

<sup>2</sup>Department of Mechanical Engineering, Yaba College of Technology, Yaba, Lagos, Nigeria

<sup>3</sup>School of Mechanical Engineering, Vellore Institute of Technology, Chennai, India

<sup>4</sup>School of Mechanical Engineering, Vellore Institute of Technology, Vellore, India

<sup>5</sup>Department of Mechanical Engineering, Lagos State University of Science and Technology, Ikorodu, Lagos, Nigeria

\*Corresponding author: sa\_oke@yahoo.com

## Article history

Received

3<sup>rd</sup> March 2025

Revised

30<sup>th</sup> December 2025

Accepted

3<sup>rd</sup> February 2026

Published

30<sup>th</sup> May 2026

## ABSTRACT

*Vibration in rotating and reciprocating machines and structures will likely increase with machine age and prolong machine usage. Thus, converting such a threat to machines for an opportunity in innovative energy harvesting is a unique advantage to industrial decision-makers. This study optimises the energy harvesting parameters of a piezoelectric cantilever-based system using the Box Behnken Design (BBD) Methodology to provide a sustainable solution for energy conversion using piezoelectric materials. Literature data that distinguishes the important parameters of the systems as follows was considered: Load resistance, width of piezo-plate and length of the piezo plate. A comprehensive analysis of the parameters and responses of the optimum scheme is presented. The feasibility of applying the Box Behnken design as a response surface approach was ascertained. BBD approximates the process parameters as a quadratic function and uses blocks to explain results. The results show that the optimal outputs are the resonant frequency of 71Hz, voltage of 6.20v, and electric power of 1.52 mW. Compared with the Taguchi method, BBD exhibits superiority in voltage, optimised load resistance with 6.05V and 12.05, respectively. Though Taguchi exceeds BBD in electric power, and optimised width with 1.78mW and 17mm, respectively, the BBD has better precision. Further studies may integrate multicriteria methods with the BBD method. The current research offers evidence of the optimisation behaviour of the piezoelectric cantilever-based energy harvester, impacting the conversion of the negative aspect of vibrations into a positive form for industrial equipment sustainability. The results emphasise the urgent need for interventions and policies to improve industrial management.*

**Keywords:** Box Behnken Design, Experimental Design, Energy, Rotating machines

© 2026 Penerbit UTM Press. All rights reserved

## 1. INTRODUCTION

Rotating and reciprocating machines and systems are significant sources of vibrations [1 - 3]. Rotating machines and systems, such as turbines, pumps and gears experience misalignments and even loading, causing vibrations, which could be very disturbing, counter-productive and very costly to control [4, 5]. In essence, the unbalanced forces produced by operating mechanisms and dynamically unbalanced masses are the greatest sources of vibration which should be controlled and may be converted into useful innovative technologies [6, 7]. However, for decades, the control mechanism has included process redesign and the introduction of damping systems which are very costly to maintain in the face of growing economic difficulties in industrial enterprises [8, 9]. Furthermore, the amazing and unprecedented innovations and technologies available for energy harvesting have evolved as a game changer in the management of vibrations [10, 11]. Interestingly, Liu [10] demonstrated the utility of a vibration-mitigation and energy-harvesting system in a dual objective device to establish the validity of a generic model. Li [11] proposed a system that simultaneously suppresses vibration and harvests vibration energy with optimal outcomes, validating the approach in a convergence scheme. Therefore, to ensure that vibrating systems are optimised, using vibrations to produce electrical energy for energy harvesting is a compulsory requirement [10, 11].

### 1.1 Some research articles published on the applications of piezoelectric harvesting principles in engineering and applied sciences

In the following reviews, some relevant papers on the piezoelectric harvesting system applications are presented. Le [12] designed and calculated the piezoelectric harvester's biomorph circular diaphragm using finite element analysis (ANSYS). The study suggested the optimal structure of the harvester based on the obtained frequency and optimal load. For this study, the effectiveness of the piezoelectric harvester is dependent on frequency. Liao et al. [13] developed a nonuniform piezoelectric bending beam based on energy harvested from the human knees and also optimised the shape of the harvested to improve the harvesting rate. It reported an experimental testing on three subjects. This research is limited to applications in the kneel of the human body for application. Hence, it cannot be applied to the other parts of the human body. Research by Alzuwayer et al. [14] aimed at optimising the basic cantilever harvester parameters to maximize energy production without much focus on the frequency. The simulation was carried out using ANSYS. This research focused on average power generation which can be affected by various environmental frequencies. Xu et al. [15] paper presented a design of a stacked piezoelectric harvester to capture the pressure pulsation in a water hydraulics system. This paper also responded that voltage increased with increased pressure amplitude. The performance is highly dependent on pressure pulse rates. Zheng et al. [16] reviewed the state-of-the-art piezoelectric wind harvester advances. It introduces its principles of operations and classifications. This study is limited to wind energy harvesting review.

Parvathi et al. [17] introduced a novel micro electrical, mechanical system harvester, rectangular with a triangular tip shape. The results were obtained from simulations using COMSOL Multiphysics. It also reported that this shape creates more stresses at the tip while generating useful voltage and power. It is particularly focused on the novel shape proposed and might not be achievable. Aceti et al. [18] reported a novel development on the based mechanism for harvesters while studying the effect of the impacting mass on a cantilever piezoelectric transducer. It also analysed impacts at the cantilever tip without the tip mass yielding the most effective configuration. The performance of this approach is highly dependent on impact position and configuration. Hu et al. [19] presented a novel topology optimisation of a multi-resonant piezoelectric

harvester while aiming to generate constant power output over a range of frequencies hence being able to operate under any condition. This research is also limited to the material chosen. Li et al. [20] research proposed a tuneable stable energy harvesting system while varying two parameters. This study also used a genetic algorithm to optimise the models chosen and determined the sensitivity of each of the selected parameters. The optimal model might not be readily available due to material choice. Liao et al. [21] focused on harvesting energy from a human knee using a piezoelectric harvester. The harvester was designed and optimised to enhance its performance. This study reported experimentation of the optimised harvester on subjects and recorded the maximum generated power as 22.55mW while waking. The research application is limited to the knees.

## 1.2 Observations, research gap, motivation and research novelties

Notwithstanding, within the research area corresponding to energy harvesting from systems, the primary focus is optimising parameters. While this research endeavour has been fruitful, the Taguchi method used to achieve this goal is limited and has been criticised for its inability to specify the correct dimensions of parameters in optimisation. Therefore, decision-making based on the Taguchi method has drawbacks that should be corrected urgently. Thus, using the Box Behnken design method with features to overcome the abnormalities of the Taguchi method may be appropriate to solve this problem.

Considering Ismail and Husaini [22], the Taguchi method succeeded in energy harvesting practices. In the scheme, a two-way biomorph cantilever that comprises two materials namely structure steel and lead zirconate titanate was the subject of an investigation into a design implemented in COMSOL software. The success of the Taguchi method may have been driven by its experimental design capability, which allows the accomplishment of a few experiments while permitting several inputs, moreover, the input parameters have several levels. However, to overcome the drawbacks of the Taguchi method stated earlier, the Box Behnken design method has been deployed to produce a highly reliable biomorph cantilever. Structural steel and lead zirconate titanate are important materials used in this work. Moreover, several studies have been conducted on this subject to date. However, it is surprising to note the absence of publications on optimising parameters of the piezoelectric cantilever-based energy harvester using the Box Behnken design method. Given that the Box Behnken design method has several advantages but they have not been explored for the problem being considered here.

This study therefore focuses on the optimisation behaviour of responses and parameters of the energy harvesting system, through a piezo-electric cantilever structure using data from Ismail and Hussein [22] which emphasized the optimisation of responses and parameters using the Taguchi method. While the most relevant work to this study, Ismail and Hussein [22] examined and organized the orthogonal arrays in alignment with parameters and their levels to reduce the required number of combinations to be tested using an alternative factorial design method, it cannot avoid extreme treatments combinations which is a merit of the Box Behnken Design used in the present study. This study addressed this gap in the literature by introducing the Box Behnken Design (BBD) method. By using the BBD method, the present study intends to contribute a deep insight into the optimisation potentials of the parameters of the energy harvesting process thus creating an opportunity for improved planning during the design and development process.

This paper is motivated by the desire of the authors to solve the crucial energy challenge faced by the manufacturing industry nowadays. The industrial sector has a heavy reliance on energy to function. The industry operates complicated heating and cooling processes, as well as machines such as conveyor belts and cutting tools. In all these processes, efficient energy control and utilization are critical to maintaining the economic growth of the manufacturing industry. A principal concern in this perspective is that energy costs must be minimized. Concurrently, efficient maintenance strategies are expected on

the rotary and reciprocating machines which combine energy but also generate vibrations. These vibrations are waste that is often overlooked but are critical in producing harvests using energy, which could complement the existing energy supply and promote cost-effectiveness in the manufacturing industry. Recognizing this operational gap within the plant, this study introduces a new method by quantitatively associating the vibrations to an optimised energy harvest system. The principal novelty and motivation of this research are as follows:

- This research uniquely analyses the optimisation thresholds using the Box Behnken Design approach, for a piezoelectric cantilever-based energy harvesting system. This is a critical approach to utilizing vibration effects on the machines in the manufacturing system.
- Unlike existing research, which utilizes the Taguchi method whose optimised values for parameters are difficult to relate to one another regarding superiority, the present study contributes a framework that overcomes the drawback.

## 2. METHODOLOGY

### 2.1 Basis to select the energy harvesting system factors

This section offers information on the essential basis for selecting the piezoelectric cantilever energy harvesting (PCEH) system factors used in this work. However, to understand the idea analysed here, the goal of the PCEH system should be put into perspective. Moreover, the goal of the PCEH system which the energy policy community should aim at to evaluate the failure or success of the PCEH system, is to transform atmospheric vibrational energy from the surroundings into disposable electrical energy. This is accomplished by employing piezoelectric influences. The scenario entails converting mechanical stress on a piezoelectric material into electrical charges. The mechanism takes advantage of the bending motion experienced by the cantilever beam structure. This is called energy harvesting of the output and is useful for low-power electronic devices such as sensors and wireless transmitters. This power of the device eliminates the necessity for other power sources.

In PCEH systems, activities are usually in four phases: In the first phase, the piezo element produces an alternating current voltage from the influence of mechanical stress. The second phase engages the rectifier that transforms the alternating current voltage to the direct current voltage. The third phase involves the regulator to ensure stable delivery of power despite load fluctuations in the circuit. The fourth phase activates capacitors and batteries, which store energy in the form of electrostatic charges on plates but electrochemical processes are used by batteries. More processes are used by batteries. Moreover, in PCEH systems, system failures due to load and the performance of the piezoelectric plate are a foremost hindrance to attaining the translation of vibrational energy into electrical energy and a major challenge to the economic sustainability of the system. Furthermore, the load in harvesting systems is controlled by the power management of the harvested energy's flow, matching the connecting device's demand and ascertaining optimal use of the captured energy. However, the relationship between load and resistance in the system is crucial to the effective management of load. If load resistance is high less current will flow through it, serving as an effective control mechanism.

Therefore, load resistance was chosen as a key representative factor for the good maintenance of the PCEH system. This choice is consistent with the proposition in Ismail and Husaini [22] which chooses it as one of the key factors of the PCEH system. In addition, the performance of the piezoelectric plate is a key determinant in the success or failure of the PCEH systems. However, the piezoelectric plate has two major dimensions, notably its

length and width. It is known that if the length of the piezoelectric plate increases, a surge in energy output is likely. Moreover, higher energy outputs are expected from widening the piezoelectric plate. It implies that the mechanical stress increases the effective surface area and large electrical charges in the piezoelectric influence will likely be experienced. Therefore, considering the influences of the plate's width and length on the electric energy generation, coupled with load resistance, significant focus on these three factors is essential to monitor the performance of the PCEH system.

## 2.2 Design of Experiment using Box Behnken Response Surface Method

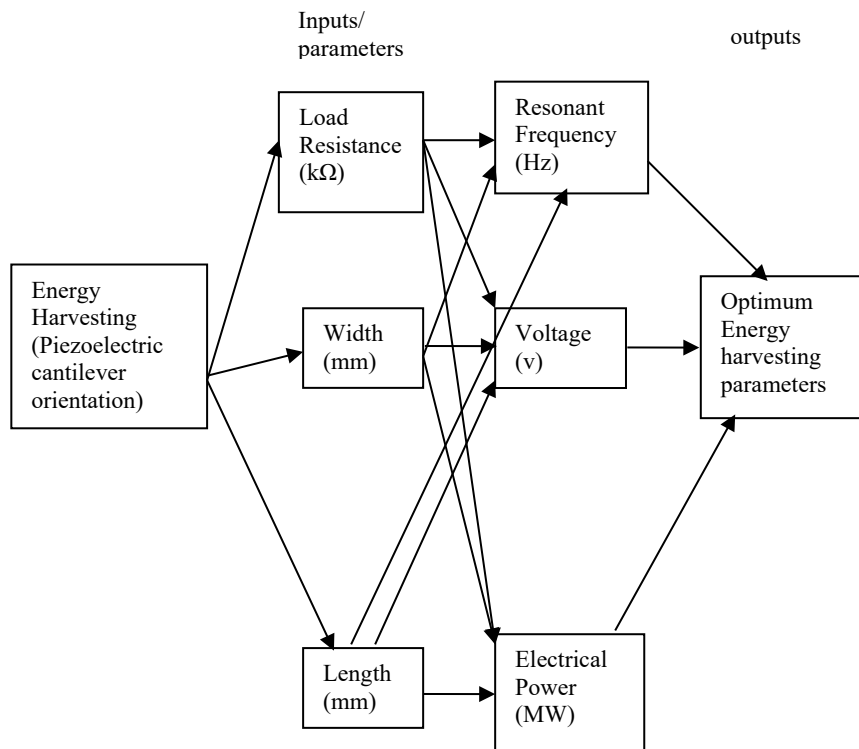
The three major parameters considered are the width of the piezoelectric plate, its length and the load resistance which has a massive effect on the output with three levels for each parameter. The Box Behnken's response surface method was used in this experimental design. The response surface method or RSM is a collection of mathematical and statistical techniques used for the design of experiments and analysis of multi-level factors and levels whose objective is to optimise this response. Box Behnken RSM reduces the number of experiments needed to find the optimal response or design parameters. The factors and levels are shown in Table 1, while the experimental order is shown in Table 2. The effect of varying these parameters (Load, Piezoelectric width and Piezoelectric length) on the voltage(v)and electrical power output(MW) is studied and presented in the results and discussion section.

**Table 1: Factors and Level [22]**

S/N	Factors	Levels		
		1	2	3
1	Load resistance (kΩ)	11	13	15
2	Width of piezoelectric plate (mm)	13	14	16
3	Length of piezoelectric plate (mm)	21	22	23

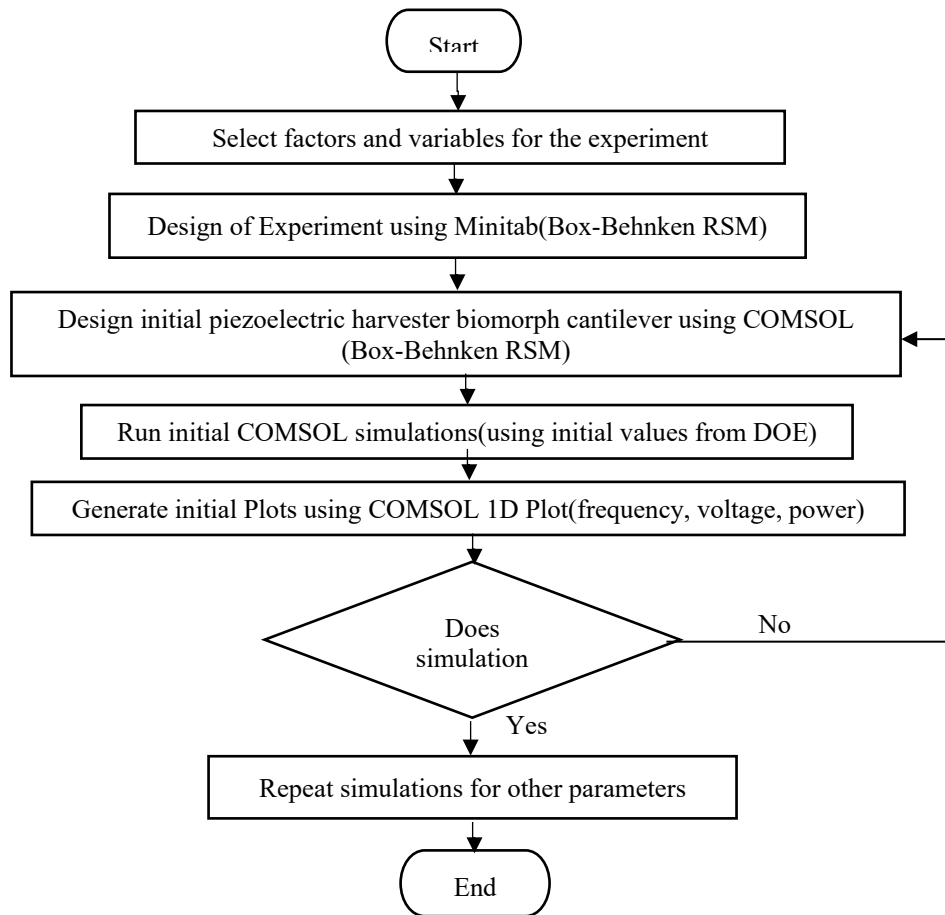
In this article, experimental design is deployed, which compels the researcher to define the system as factors, these are the independent variables that are controlled for the measurement of the system goals. The factor is studied to examine how it influences the outcome of the energy harvesting system. However, to proceed on an experimental design mission where the orthogonal array and the average signal-to-noise ratios are computed, levels must be defined. Levels take the form of members, continuous or non – continuous. Descriptions of system characteristics, which appear in different forms can be converted to levels. Additionally, several measures of the parameters may be grouped and each group represents a level in the factor-level consideration. In order to illustrate how Table 1 was obtained, Ismail and Husaini [22] used COMSOL software, which measured each of the parameters. To illustrate the reading of the loud resistance parameters, the current flow is simulated through the wire geometry. By applying material characteristics such as resistivity, the voltage drop across the wire is computed. Then Ohm's law is applied to establish the resistance given the knowledge of the researcher on the current and voltage that are simulated. The simulations may be conducted on 50 occasions. Then the ranges of the numbers are used to group the simulations into three groups, for instance. The averages of each group are then used to represent the load resistances of interest. The selection of 50 occasions for the simulation being described is based on a practical choice. It is guided by statistical rules of thumb, which declare a value of at least 30 occasions in simulation as large and representative of samples. This is further justified by the computational constraints and the preferred degree of result precision [22]. The same approach could be taken for the measurements of other parameters into levels.

Figure 1 shows the interrelationships of the inputs and outputs of the energy harvesting system. It reveals a high-level description that provides insights into the optimisation process. It shows how the inputs are represented, transformed and controlled to the resonant frequency, voltage and electric power.



**Figure 1:** Energy Harvesting (Piezoelectric cantilever-based convention)

Figure 2 is a flow chart used to design the experiment using the Box Behnken Design method. It is a master plan which shows movement from the parametric selection stage to a proven stage of optimisation, presented systematically and insightfully. The step-by-step guidance demonstrated in Figure 2 consists of the preliminary stage, where the principal operating parameters are identified. At this stage, the parameters having the greatest impact on the harvesting systems' outputs are defined. Next is the concern for experimental run minimisation, the design of experiments shows how to structurally determine a reduced number of experiments that is economically preferred to full factorial designs. This is linked to the COMSOL model to establish a predictive model, which maps the experimental result steps. The outcome of this exercise is the developed mathematical model that associates each of the inputs (load resistance, width and length) to outputs (resonant frequency, voltage and power). Then, the optimal conditions are sought for. This is achieved from a combination of the model and the plots, which guide the choice of particular input parameters that may produce the optimal outputs. A principal advantage of using the BBD model is that it avoids producing impractical or unsafe extreme conditions that trigger system failure. It avoids the concurrent testing of the parameters at high or low extremities. The concluding phase is the validation of the predicted results, which confirms the accuracy of the developed model [23-27].



**Figure 2:** Flow chart of process

Table 2 is the transformed form of Table 1 when the orthogonal array is applied. However, the orthogonal array is not shown in this work but its application is explained to understand how to proceed from Table 1 to Table 2. The orthogonal array used in the work consists of 15 experiments, indicating 15 rows of entries where each entry has three items, 1, 2 and 3. The values, 2 and 3 represent each parameter of load resistance, width and length respectively. Notice that the use of an orthogonal array is to provide a safe ground for experimentation with the use of fewer experimental trials instead of factorial experiments that account for all tests of possible options. For Table 2 to be understood, consider the second column, which represents the cells containing orthogonal entries for the load resistance alone. In this situation, all the 15 entries of 1, 2 and 3 must be part of a larger orthogonal matrix that accounts for all the factors. Consider entries 1, 2 and 3 under the load resistance column of Table 2. The values there are 11, 15 and 15. It means that the orthogonal array from the original matrix shows 1, 3, and 3. From Table 1, under load resistance, level 1 has an equivalence of 11, and level 3 has an equivalence of 15. Thus, in Table 2, the first three entries corresponding to 1, 3 and 3 are 11, 15 and 15. The same logic is used to fill Table 2 when the orthogonal array is extracted from predefined tables such as those obtainable in Minitab 18 (2020) software.

**Table 2:** Box Behnken Design of Experiment

Experiment Number	Load Resistance	Width	Length
1	11	16	22
2	15	14	21

3	15	16	22
4	11	13	22
5	11	14	21
6	13	16	23
7	13	14	22
8	15	13	22
9	13	13	21
10	13	14	22
11	15	14	23
12	13	16	21
13	11	14	23
14	13	14	22
15	13	13	23

Table 3 shows the design summary, which offers a short outline of the experimental setup, such as the number of factors with the associated levels, the required number of runs and how the runs are arranged. It is a roadmap that provides an understanding of the experimental structure and the manner the factor combinations are tested for the effective analysis of the response surface.

**Table 3:** Design Summary

Factors:	3	Replicates:	1
Base runs:	15	Total runs:	15
Base blocks:	1	Total blocks:	1

### 3. RESULTS AND DISCUSSION

In this work, an attempt is made to evaluate the effect of changes in the load resistance, width and length of the piezoelectric harvester, on frequency, voltage and electric power generated by the harvester. The impact of varying these parameters (Load, Piezoelectric width and Piezoelectric length) on the voltage(v), mechanical power input(MW) and electrical power output (MW) were studied and the results are presented below. Table 4 shows the effect of varying the input parameters (load, width and length) on the outputs (resonant frequency, voltage, mechanical power and electrical power). Figure 3 to 20 shows various plots which detail the relationship between input parameters and factors. These plots were obtained by simulations. Different computations of Analysis of variances (ANOVA) were generated to determine the significance of each input parameter on the output.

**Table 4:** Effect of varying input parameters on output parameters

Experimental No.	Input parameters			Output parameters		
	Load Resistance	Width of Piezoelectric Plate	Length of Piezoelectric Plate	Resonant Frequency (Hz)	Voltage (v)	Electrical Power Out (mW)
1	11	16	22	65	5.6644898	1.458474771
2	15	14	21	71	5.6234297	1.054098705
3	15	16	22	66	6.1985565	1.280736748
4	11	13	22	65	5.3726656	1.312069785
5	11	14	21	71	5.1360972	1.199067911
6	13	16	23	60	6.1335696	1.446949102
7	13	14	22	65	5.7049939	1.25180599

8	15	13	22	65	5.7829376	1.114745593
9	13	13	21	71	5.2991829	1.080051497
10	13	14	22	65	5.7049939	1.25180599
11	15	14	23	60	6.1420246	1.257482225
12	13	16	21	71	5.6109596	1.210879511
13	11	14	23	60	5.7902762	1.523968118
14	13	14	22	65	5.7049939	1.25180599
15	13	13	23	60	5.9115205	1.344079797

Table 4 shows the values of the outputs (frequency, voltage and electrical power generated from the input parameters (load, piezoelectric width and piezoelectric length). However, the first step toward determining the optimised combination of parameters is to establish which of the outputs are beneficial or non-beneficial. Considering the resonant frequency, it is a critical parameter and beneficial since it triggers the optimum achievement of efficiency and power output. The voltage is also a beneficial parameter since an increase in the voltage for a particular power threshold could yield enhanced efficiency of power. Thirdly, electric power output is considered beneficial as higher power output leads to a more effective performance of a system in powering devices. Furthermore, by visualising the values of the outputs, 71Hz of resonant frequency, 6.1985565v of voltage and 1.52396811 mW of power out are the optimal points of output in the results in Table 4. But these values do not produce a complete set of corresponding inputs. Therefore, a near-optimal value, which may be less than these stated values but with a complete set of input and output values, needs to be identified. This is obtained at experimental number 6 with inputs of 13, 16 and 23 units of load resistance, width of piezoelectric plate and length of piezoelectric plate, respectively. The corresponding outputs are 60Hz, 6.1335696v and 1.446949102 mW of resonant frequency, voltage and electric power out, respectively. Moreover, the theoretical reasoning strengthening these results lies in the efficiency of the Box Behnken Design to fit a quadratic model. This model explains the association among multiple inputs and each of the outputs. Table 4 shows information from COMSOL multiphysics software applications, on the parameters and responses of the energy harvesting system using the piezoelectric cantilever framework. The inputs from the Box Behnken Design, which searches for the best input combinations for the targeted outputs. In the present context, the best combinations of load resistance, length and width of the piezoelectric cantilever structure that yield targeted resonant frequency, electrical power and voltage are sought. These become the optimum energy harvesting parameters of the system. The combination of input parameters is also referred to as alternatives of the parameter. These give the generated outputs or responses mentioned earlier. As the values generated in Table 4 are substituted in Minitab 18 (2020) software, statistical analysis is conducted such that tables such as the ANOVA (analysis of variance) are generated.

### 3.1 Effect of varying input parameters on Resonant Frequency generated

Table 5 shows the coded coefficients for resonant frequency. In Table 5, the values of the various categories of variables in the regression model are changed by applying codes pending analysis. The outcomes are coefficients that represent the obtained differences of the response valuables for the varying levels considered. Moreover, the coded coefficient table is also generated using the Minitab software. The coded coefficient table displays values that describe the behaviour of the parameters of the energy harvesting system. A key value of interest is the coefficient (Table 5). An instance is the coefficient of the resistant frequency. In Table 5, the second column, "Coef" is the short form of coefficient and shows the predicted changes, which may be brought about when evaluating the mean for the

resonant frequency when a one-unit growth in the coded predictor is desired with the other terms remaining unchanged. The "SE Coef", which appears in the third column of Table 5, is the shortened form of the standard Error of the Coefficient. It aims to evaluate how precisely the estimated coefficient of each term can be made. These are the parameters impacting the resonant frequency. The t-value is the t-statistic that evaluates the proportion of the coefficient to its standard error. The p-value answers the question of whether the parameter considered or its interaction thereof shows a statistically significant outcome/influence on the resonant frequency. The VIF is termed the variance inflation factor, whose purpose is to estimate how much the variance arising from a regression coefficient is inflated due to the effects of multicollinearity.

**Table 5:** Coded Coefficients for Resonant Frequency

Term	Coef	SE Coef	T-Value	P-Value	VIF
Constant	65.000	0.129	503.49	0.000	
Load Resistance	0.1250	0.0791	1.58	0.175	1.00
Width of Piezoelectric Plate	0.1250	0.0791	1.58	0.175	1.00
Length of Piezoelectric Plate	-5.5000	0.0791	-69.57	0.000	1.00
Load Resistance*Load Resistance	0.125	0.116	1.07	0.332	1.01
Width of Piezoelectric Plate*Width of Piezoelectric Plate	0.125	0.116	1.07	0.332	1.01
Length of Piezoelectric Plate*Length of Piezoelectric Plate	0.375	0.116	3.22	0.023	1.01
Load Resistance*Width of Piezoelectric Plate	0.250	0.112	2.24	0.076	1.00
Load Resistance*Length of Piezoelectric Plate	-0.000	0.112	-0.00	1.000	1.00
Width of Piezoelectric Plate*Length of Piezoelectric Plate	-0.000	0.112	-0.00	1.000	1.00

Tables 6 and 7 show information on the Analysis of Variance for Frequency and Fits and Diagnostics for Unusual Observations for Frequency.

**Table 6:** Analysis of Variance for Frequency

Source	DF	Adj SS	Adj MS	F-Value	P-Value
Model	9	243.083	27.009	540.19	0.000
Linear	3	242.250	80.750	1615.00	0.000
Load Resistance	1	0.125	0.125	2.50	0.175
Width of Piezoelectric Plate	1	0.125	0.125	2.50	0.175
Length of Piezoelectric Plate	1	242.000	242.000	4840.00	0.000
Square	3	0.583	0.194	3.89	0.089
Load Resistance*Load Resistance	1	0.058	0.058	1.15	0.332
Width of Piezoelectric Plate*Width of Piezoelectric Plate	1	0.058	0.058	1.15	0.332
Length of Piezoelectric Plate*Length of Piezoelectric Plate	1	0.519	0.519	10.38	0.023
2-Way Interaction	3	0.250	0.083	1.67	0.288
Load Resistance*Width of Piezoelectric Plate	1	0.250	0.250	5.00	0.076
Load Resistance*Length of Piezoelectric Plate	1	0.000	0.000	0.00	1.000
Width of Piezoelectric Plate*Length of Piezoelectric Plate	1	0.000	0.000	0.00	1.000
Error	5	0.250	0.050		
Lack-of-Fit	3	0.250	0.083	*	*

Pure Error	2	0.000	0.000		
Total	14	243.333			

**Table 7: Fits and Diagnostics for Unusual Observations for Frequency**

Obs	Resonant Frequency (Hz)	Fit	Resid	Std Resid
3	66.000	65.750	0.250	2.24
4	65.000	65.250	-0.250	-2.24

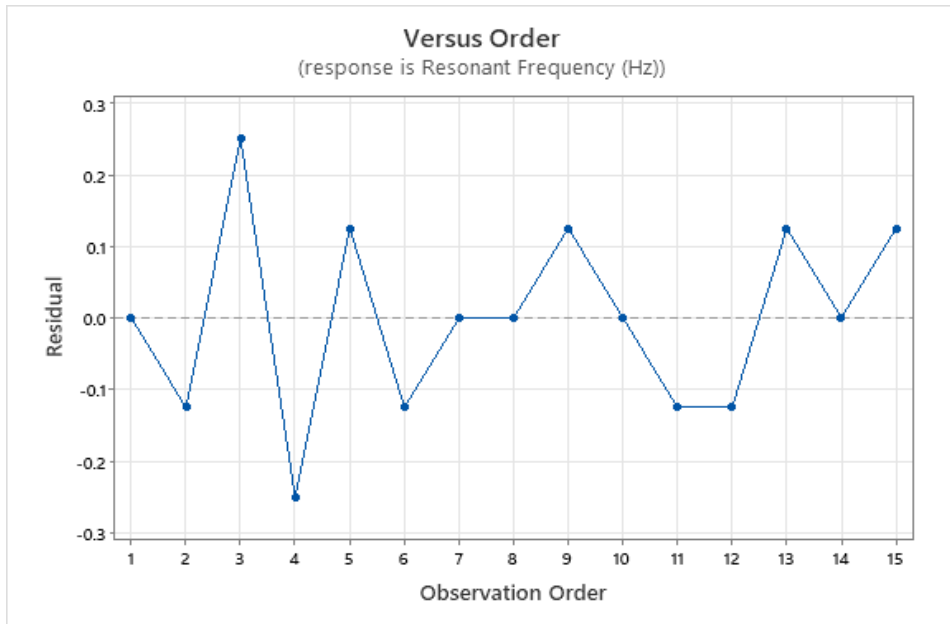


**Figure 3: Versus Order for Resonant Frequency**

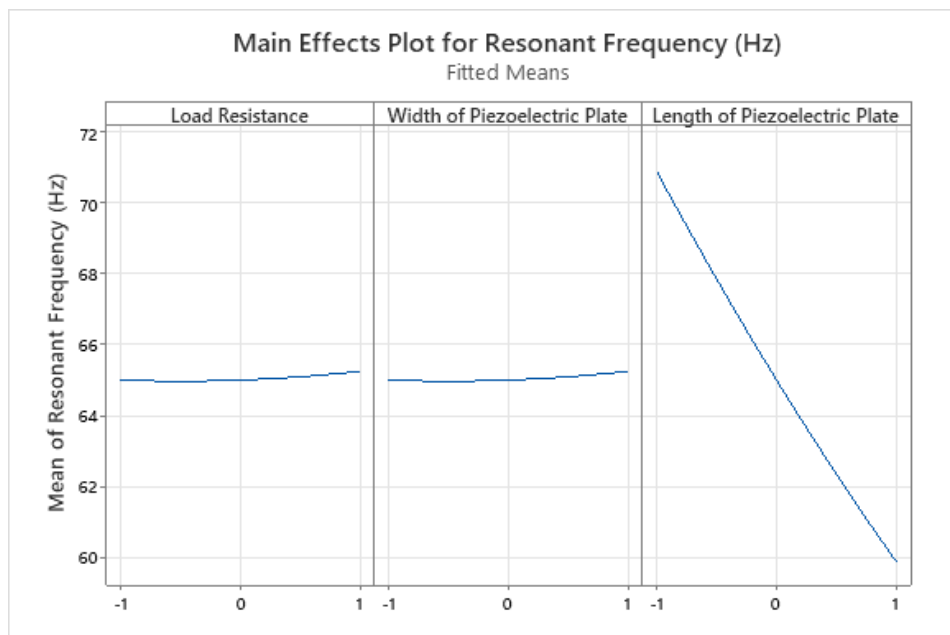


**Figure 4: Main Effect Plot for Resonant Frequency**

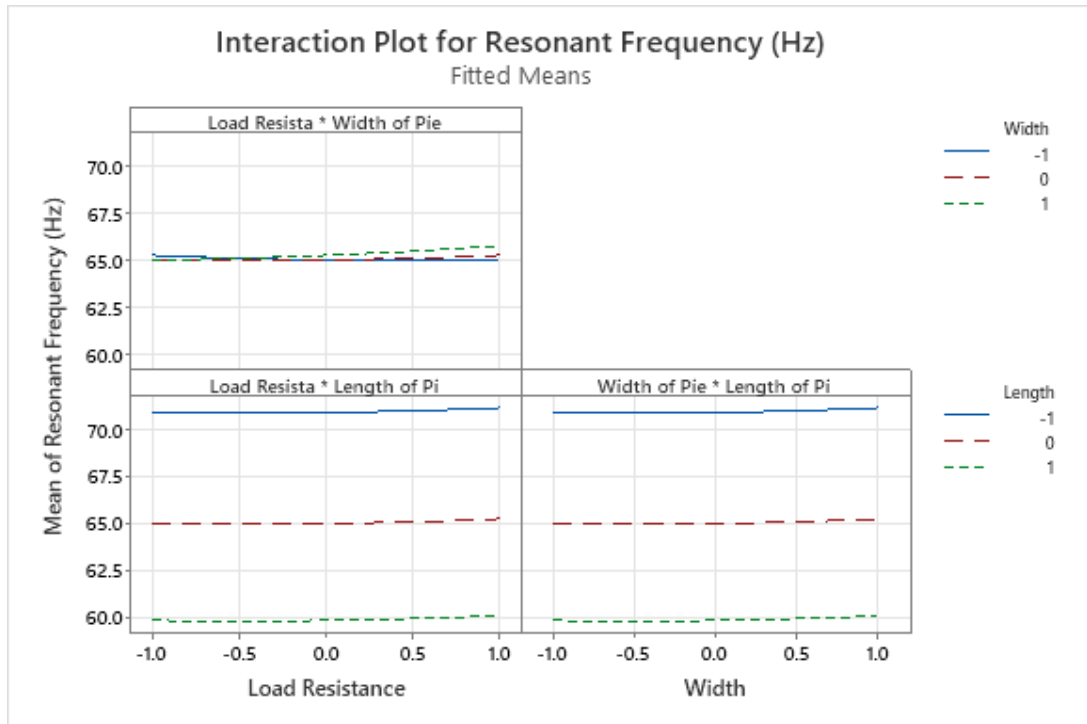


**Figure 5:** Interaction Plot for Resonant Frequency

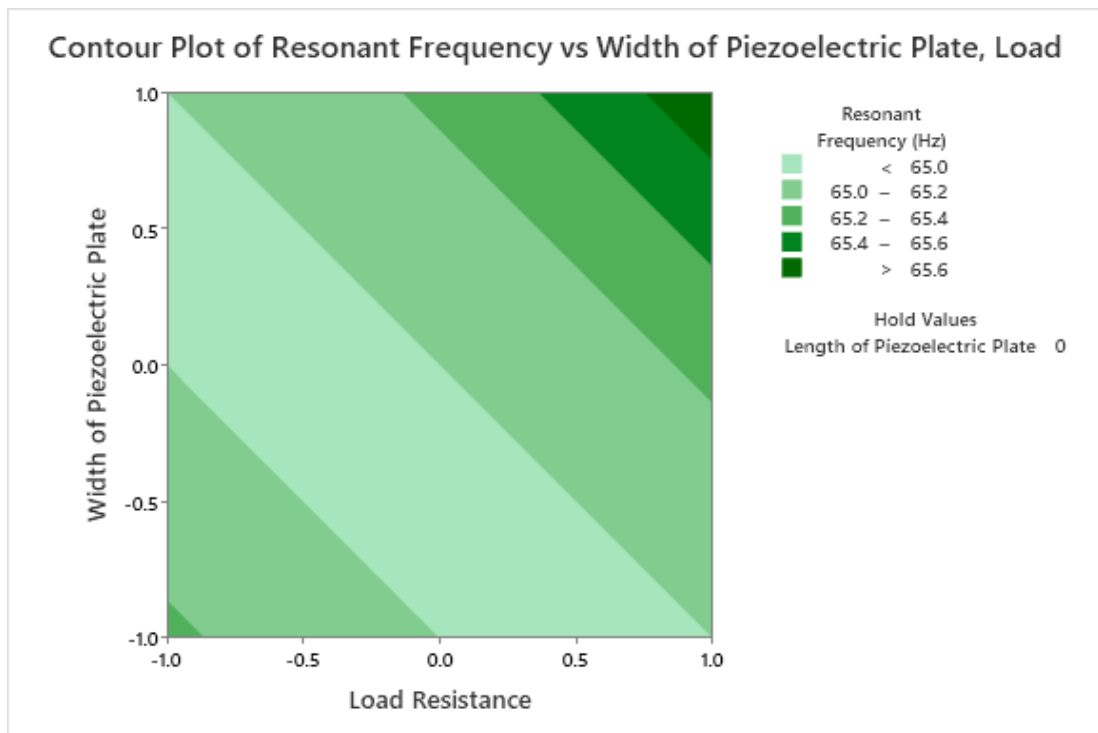


**Figure 6:** Contour Plot for Resonant Frequency vs Width and Load

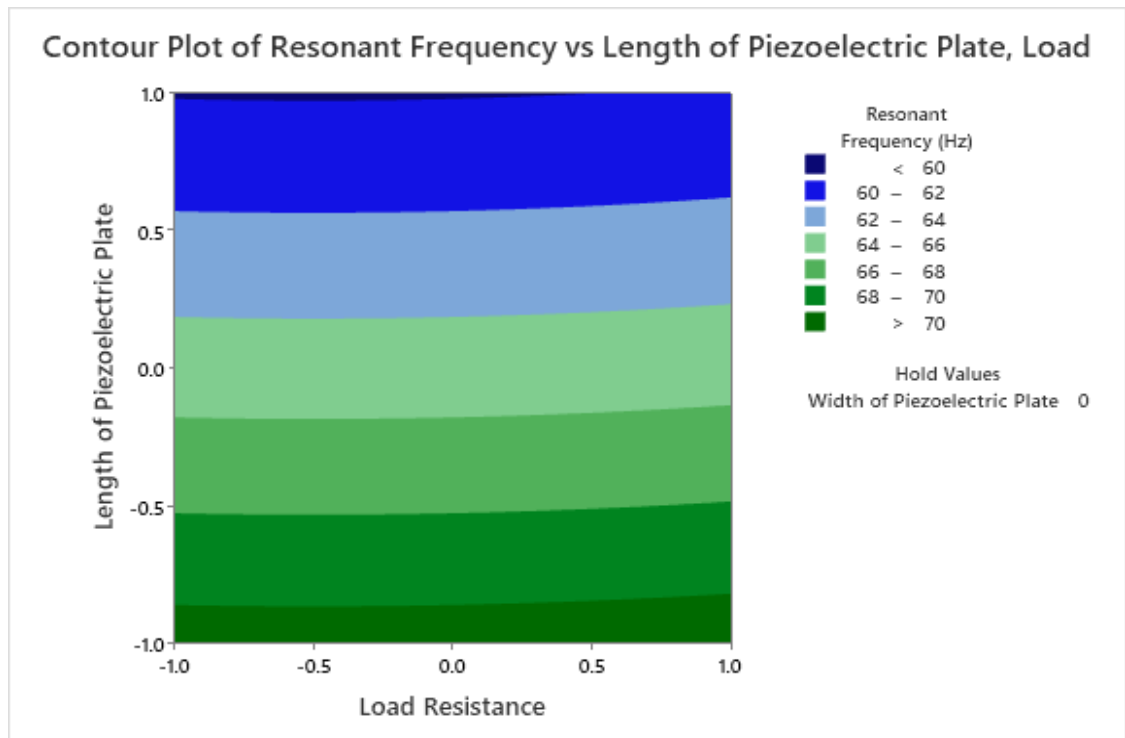


**Figure 7:** Contour Plot for Resonant Frequency vs Length and Load

Figure 7 shows the 3-dimensional surface (i.e. resonant frequency, length and load) by drawing lines which link points with similar values fixed on a 2-axis plane. It displays a top-down perspective of a surface such that lines represent areas having the same value.

Consider the negative value attached to the width of the piezoelectric cantilever, it implies that the width has a negative correlation with the frequency. The positive sign attached to the values indicates a positive correlation of the parameter with the frequency. Furthermore, the p-value shows the significant level of the particular value. Thus, for a p-value less than 0.05, the parameter considered has significance in the energy harvesting process and should be part of the predictive variables in the analysis. The statistical t-value observed could show a low or high value. However, the higher the t-value the more significant the parameter being considered is to the system. In the above discussion, the p value and t value are key elements that reflect the significance or otherwise of the parameters of the p energy harvesting process. It should be noted that the process of finding parametric significance in an energy harvesting system is called interaction. Next, the table contains constants supporting the load, resistance, width and length of the piezoelectric cantilever structure. Notice that interactions may be analyzed such as between load and load, width and load, length and load. Based on the values obtained, these mentions and interactions may or may not be significant. The ANOVA also expands the coded coefficient table. Though providing guidance similar to the coded coefficient table, the ANOVA table displays the exact p-value which is beneficial in understanding the influence of a parameter on the response measuring the system performance. To further explain the significance of the coded coefficient table, it shows that length is significant as only the p-value of length is less than 0.05 (Table 5). It is also observed that the coefficient value is also negative, which shows that length has a negative correlation (agreement) with frequency.

In practice, the interpretation of this data is that for the PZT5a piezoelectric cantilever material being worked on, the longer the length of the piezoelectric cantilever the less the frequency. By referring to Table 6 which conditions values of the analysis of

variance (ANOVA), there is the presence of F values in the table. The higher the F value the more dominant a particular parameter is on the response(s) of the process. Now, recall that the coded coefficient table declares that length is significant. However, when searching for the values of the length parameter in the ANOVA table, the F-value for length is very high, which shows that length has a dominant impact on the frequency output. This is a confirmation of the earlier results. The p-value for other parameters shows that they are not significant in frequency since they are above the p-value of 0.05.

The next table contains the error values that reveal differences in errors. The table shows that in the conducted experiments, there is an even distribution of activities, providing an equal number of values on both sides of the consideration. Moving on to the mean effect plot, the results help to confirm the declaration of the table. It shows that length carries the major difference. However, width and load did not show much difference from the midpoint line. The interaction can also be observed, which shows that the interaction is not significant. It implies there is not much difference between them. Moving forward, it is required to obtain the parameters to be optimised. From the experiment, it is observed that length is a constant value when dealing with the frequency. Considering the main effects of load and width, length is also significant. It also shows that load resistance is significant. It thus reveals a need to optimise the length since it is significant in the process. Moreover, load resistance comes into play when the voltage is considered.

Furthermore, the other situation reveals that length is major in the work. Thus, the effort now is to optimise the length and load resistance as well as the width. The goal is to find an increase in length that can yield the maximum outcome. The load effect is also to be maximized. Thus, using the Minitab 18 (2020) software, optimisation was conducted on the parameters relative to the responses. Here, length is to be maximized while the load resistance is to be reduced. Also, the width is optimised. These will yield the three unique values using the Box Behnken Design method.

### 3.2 Effect of varying input parameters on Voltage Generated

**Table 8:** Coded Coefficients for Voltage generated

Term	Coef	SE Coef	T-Value	P-Value	VIF
Constant	5.7050	0.0189	302.60	0.000	
Load Resistance	0.2229	0.0115	19.31	0.000	1.00
Width of Piezoelectric Plate	0.1552	0.0115	13.44	0.000	1.00
Length of Piezoelectric Plate	0.2885	0.0115	24.99	0.000	1.00
Load Resistance*Load Resistance	-0.0081	0.0170	-0.48	0.654	1.01
Width of Piezoelectric Plate*Width of Piezoelectric Plate	0.0578	0.0170	3.40	0.019	1.01
Length of Piezoelectric Plate*Length of Piezoelectric Plate	-0.0239	0.0170	-1.41	0.218	1.01
Load Resistance*Width of Piezoelectric Plate	0.0309	0.0163	1.90	0.117	1.00
Load Resistance*Length of Piezoelectric Plate	-0.0339	0.0163	-2.08	0.093	1.00
Width of Piezoelectric Plate*Length of Piezoelectric Plate	-0.0224	0.0163	-1.37	0.228	1.00

**Table 9:** Analysis of Variance for Voltage generated

Source	DF	Adj SS	Adj MS	F-Value	P-Value
Model	9	1.28203	0.142448	133.59	0.000
Linear	3	1.25586	0.418621	392.58	0.000
Load Resistance	1	0.39757	0.397573	372.84	0.000

Width of Piezoelectric Plate	1	0.19259	0.192594	180.61	0.000
Length of Piezoelectric Plate	1	0.66570	0.665697	624.29	0.000
Square	3	0.01572	0.005241	4.92	0.059
Load Resistance*Load Resistance	1	0.00024	0.000242	0.23	0.654
Width of Piezoelectric Plate*Width of Piezoelectric Plate	1	0.01232	0.012318	11.55	0.019
Length of Piezoelectric Plate*Length of Piezoelectric Plate	1	0.00212	0.002117	1.99	0.218
2-Way Interaction	3	0.01044	0.003480	3.26	0.118
Load Resistance*Width of Piezoelectric Plate	1	0.00383	0.003831	3.59	0.117
Load Resistance*Length of Piezoelectric Plate	1	0.00460	0.004596	4.31	0.093
Width of Piezoelectric Plate*Length of Piezoelectric Plate	1	0.00201	0.002013	1.89	0.228
Error	5	0.00533	0.001066		
Lack-of-Fit	3	0.00533	0.001777	*	*
Pure Error	2	0.00000	0.000000		
Total	14	1.28736			

**Table 10:** Fits and Diagnostics for Unusual Observations for voltage

Obs	Voltage(v)	Fit	Resid	Std Resid	
3	6.1986	6.1637	0.0349	2.14	R
4	5.3727	5.4075	-0.0349	-2.14	R

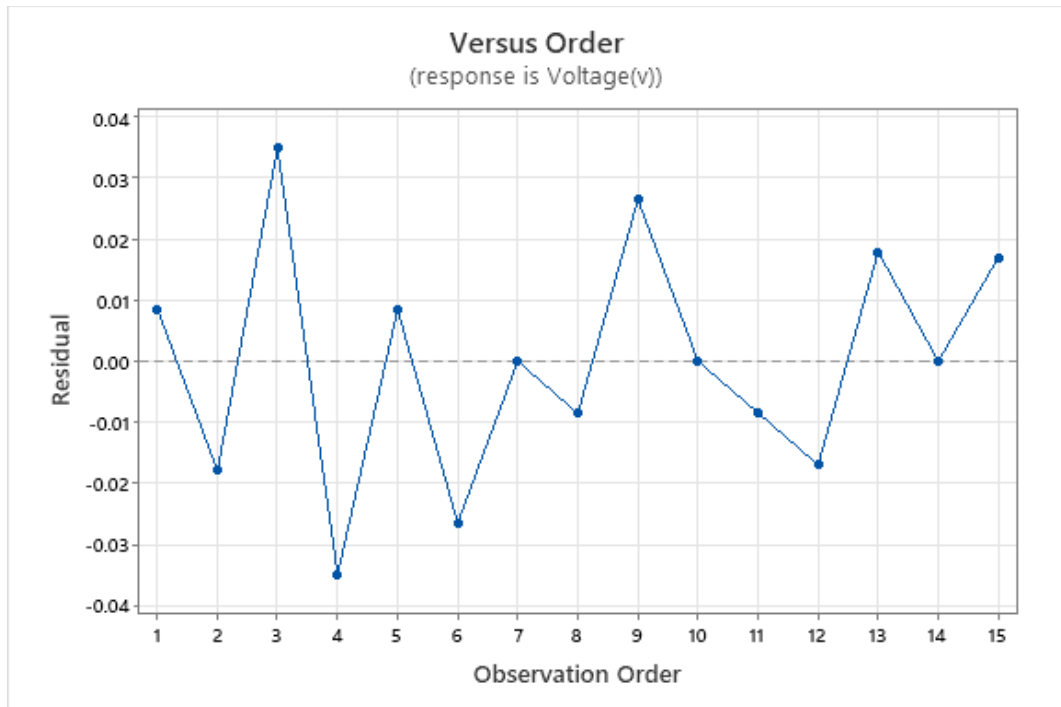


**Figure 8:** Versus order for Voltage generated

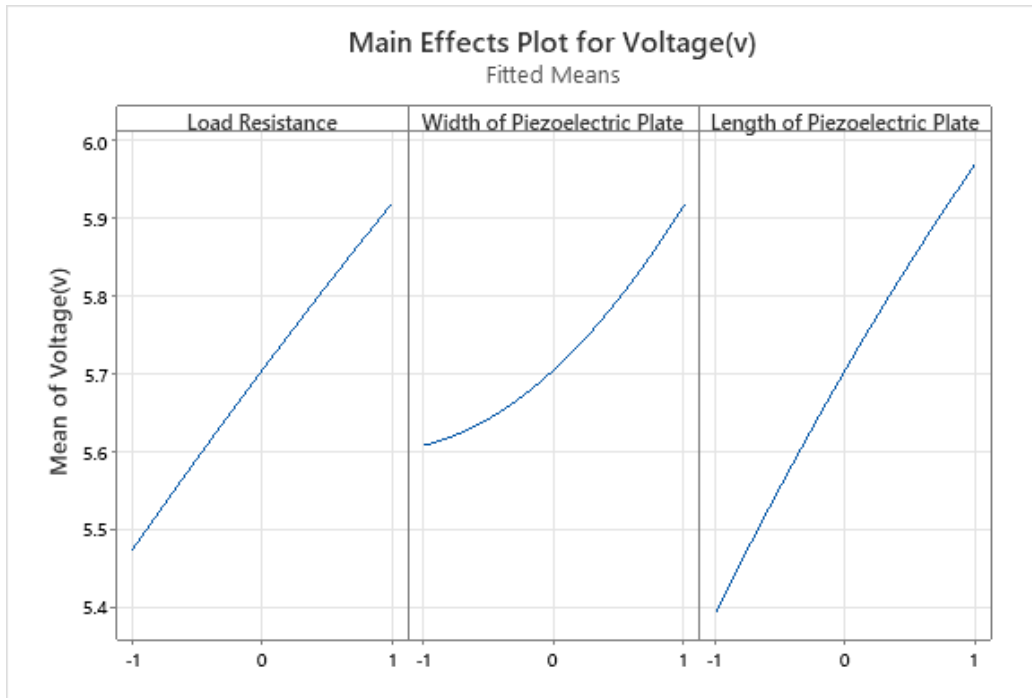


**Figure 9:** Main Effect plot for Voltage

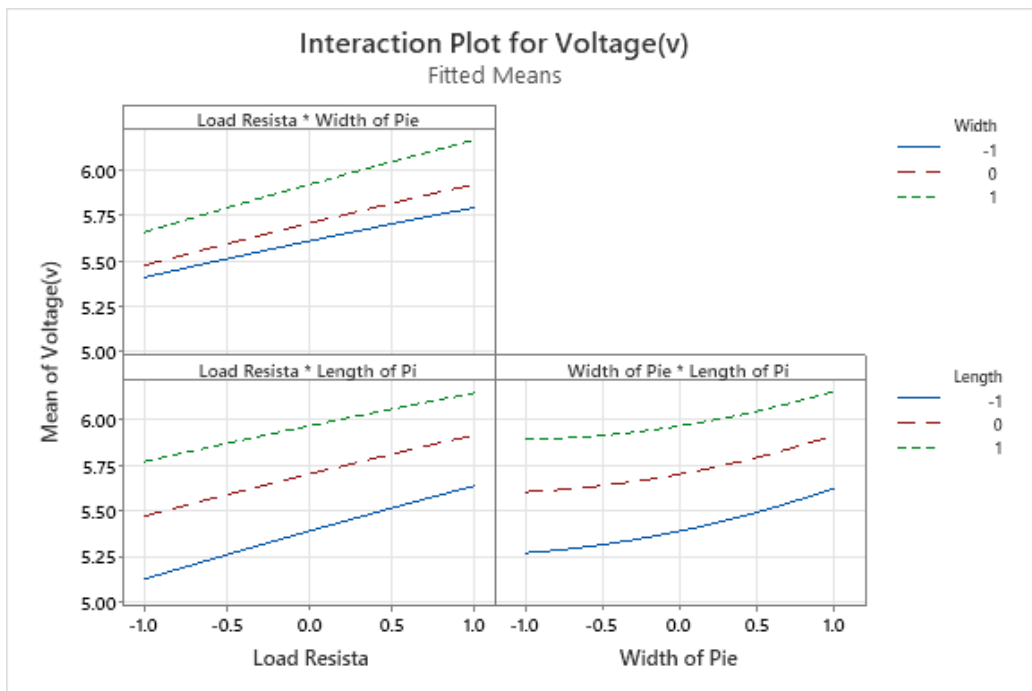


**Figure 10:** Interaction Plot for Voltage

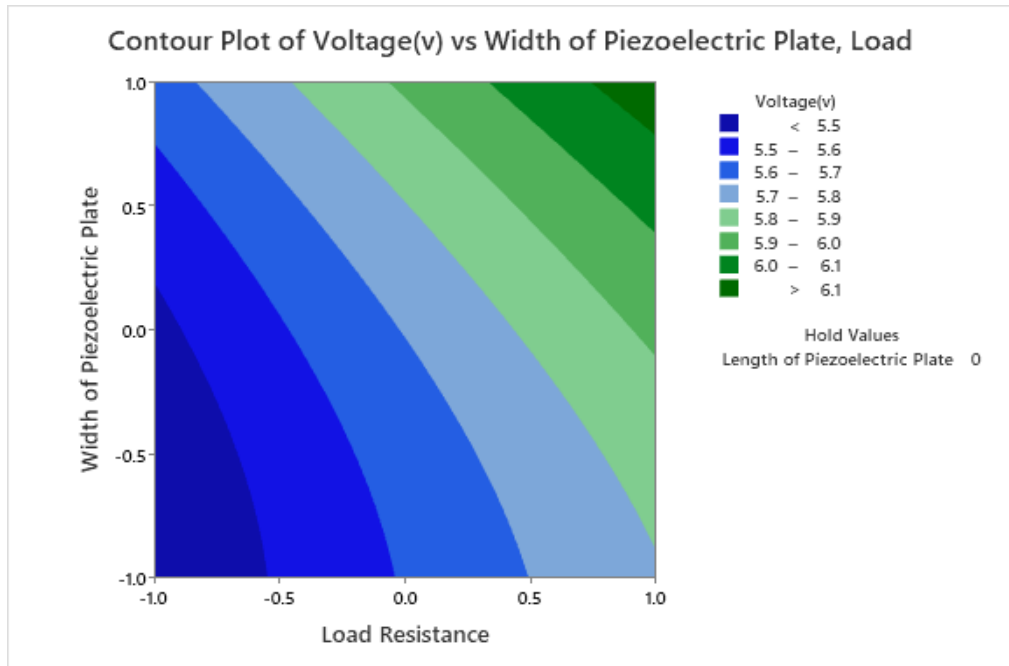


**Figure 11:** Contour Plot for Voltage vs Width and Load

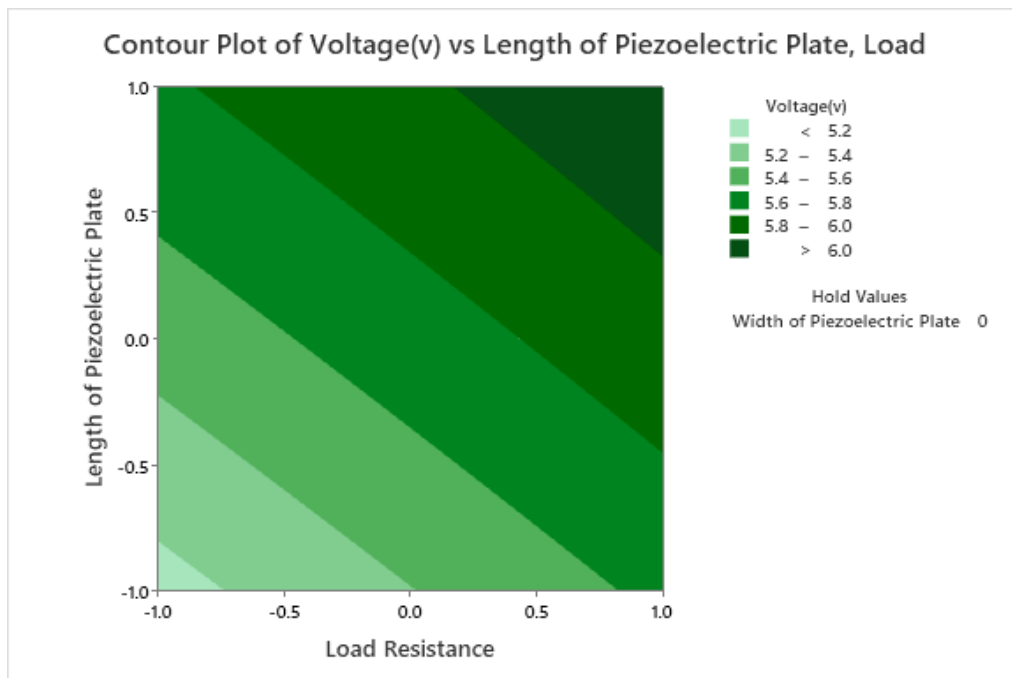


**Figure 12:** Contour Plot for Voltage vs Length and Load

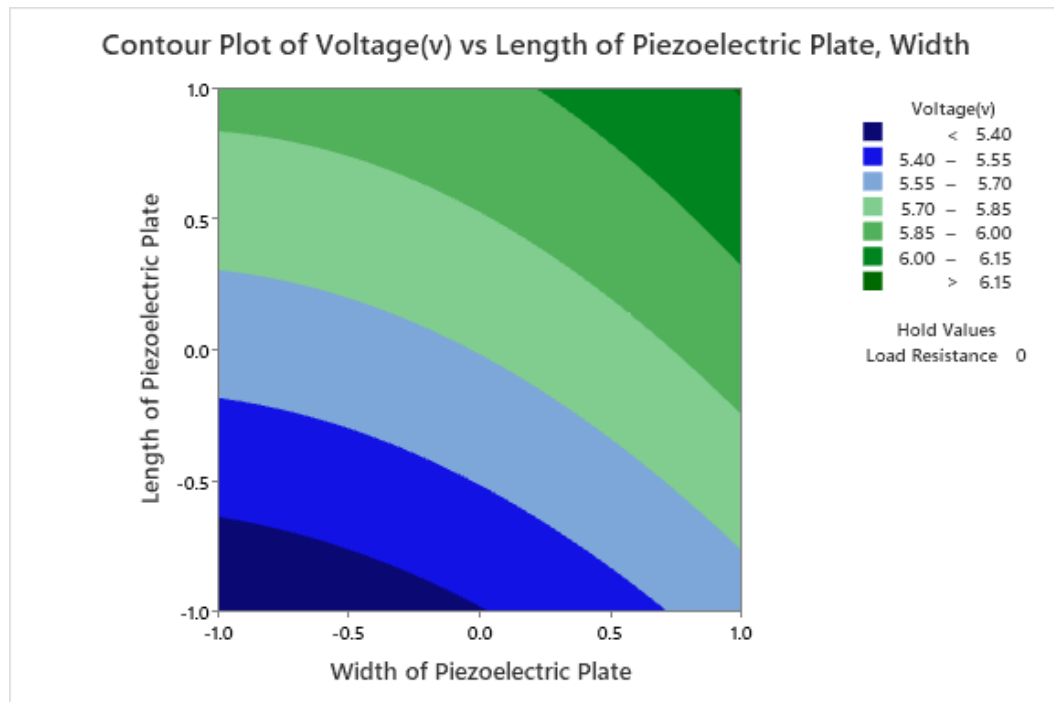


**Figure 13:** Contour Plot for Voltage vs Length and Width

The coefficient values for all three factors (load, length and width) in Table 8 are all positive suggesting a direct relationship between the voltage and the three factors. The high T-value for load, length and width coupled with the low p values ( $p \approx 0.000$ ) for the factors indicates that all three parameters are statistically significant. The F-value on the ANOVA table in Table 9 is positively high which suggests that they have a strong statistical effect on the voltage with the length having the strongest effect. The P-value on the ANOVA table also shows the statistical significance of the three factors.

It is also observed from the main effect plot in Figure 9 for voltage that three input parameters affect the voltage significantly with the length having a more significant effect on the voltage generated. Hence, with an increase in the length, width and load there is an increase in the voltage which suggests a direct proportionality. The interaction plot in Figure 10 shows that the interaction between load & width and load width & length are statistically significant which is also seen on the contour plots for voltage vs length & width in Figure 13 and voltage vs width and load in Figure 11.

### 3.3 Effect of varying input parameters on Electric power Generated

The coefficient value for electrical power generated in Table 11 has a negative value while width and length have a positive value indicating a direct relationship between electrical power and (width and length) and an inverse relationship with load. Table 11 shows the coded coefficients for electrical power, which starts with the intercept of 1.25181 Hz. The coefficient for load resistance is -0.09831, which implies that a growth in coded load resistance in a unit measure, and an expected decline by -0.0983/ unit in the electric power is expected when the width and length of the piezoelectric plate, and other parameters below the length of the piezoelectric plate in the table are constant. Table 12 shows the analysis of variance for electric power.

**Table 11:** Coded Coefficients for Electrical Power

Term	Coef	SE Coef	T-Value	P-Value	VIF
Constant	1.25181	0.00832	150.41	0.000	
Load Resistance	-0.09831	0.00510	-19.29	0.000	1.00
Width of Piezoelectric Plate	0.06826	0.00510	13.39	0.000	1.00
Length of Piezoelectric Plate	0.12855	0.00510	25.22	0.000	1.00
Load Resistance*Load Resistance	0.01393	0.00750	1.86	0.122	1.01
Width of Piezoelectric Plate*Width of Piezoelectric Plate	0.02577	0.00750	3.43	0.019	1.01
Length of Piezoelectric Plate*Length of Piezoelectric Plate	-0.00708	0.00750	-0.94	0.388	1.01
Load Resistance*Width of Piezoelectric Plate	0.00490	0.00721	0.68	0.527	1.00
Load Resistance*Length of Piezoelectric Plate	-0.03038	0.00721	-4.21	0.008	1.00
Width of Piezoelectric Plate*Length of Piezoelectric Plate	-0.00699	0.00721	-0.97	0.377	1.00

The P-value for all three factors ( $p \approx 0.000$ ) indicates are statistically significant. The high F-value on the ANOVA table indicates that the three factors have a high effect on the electric power with length having the major effect. Table 12 is the Variance for Electric power.

**Table 12:** Analysis of Variance for Electric power

Source	DF	Adj SS	Adj MS	F-Value	P-Value
Model	9	0.254132	0.028237	135.88	0.000
Linear	3	0.246800	0.082267	395.87	0.000
Load Resistance	1	0.077326	0.077326	372.10	0.000
Width of Piezoelectric Plate	1	0.037277	0.037277	179.38	0.000
Length of Piezoelectric Plate	1	0.132196	0.132196	636.14	0.000
Square	3	0.003350	0.001117	5.37	0.051
Load Resistance*Load Resistance	1	0.000717	0.000717	3.45	0.122
Width of Piezoelectric Plate*Width of Piezoelectric Plate	1	0.002452	0.002452	11.80	0.019
Length of Piezoelectric Plate*Length of Piezoelectric Plate	1	0.000185	0.000185	0.89	0.388
2-Way Interaction	3	0.003983	0.001328	6.39	0.037
Load Resistance*Width of Piezoelectric Plate	1	0.000096	0.000096	0.46	0.527
Load Resistance*Length of Piezoelectric Plate	1	0.003692	0.003692	17.76	0.008
Width of Piezoelectric Plate*Length of Piezoelectric Plate	1	0.000195	0.000195	0.94	0.377
Error	5	0.001039	0.000208		
Lack-of-Fit	3	0.001039	0.000346	*	*

Pure Error	2	0.000000	0.000000		
Total	14	0.255171			

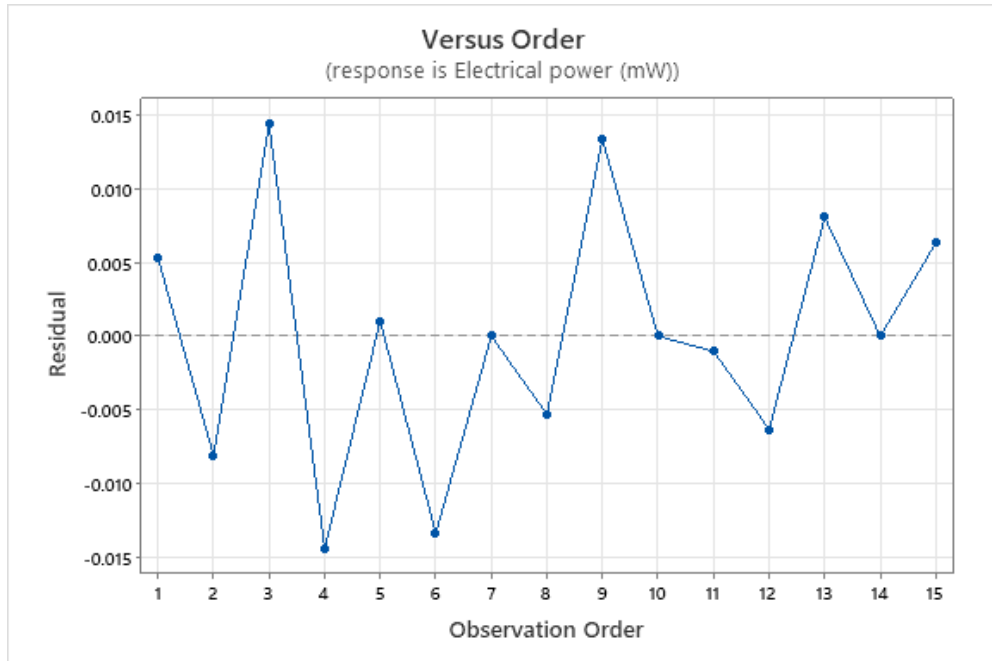


**Figure 14:** Residual Versus order for Electric power

Figure 14 is the Residual Versus order for Electric power. Figure 15 is the main effect plots for electric power. Figure 16 is the interaction plots for electric power. Figure 17 is the Contour Plot of Electric power vs Width and Load. Figure 18 is the Contour Plot of Electric power vs Length and Load.

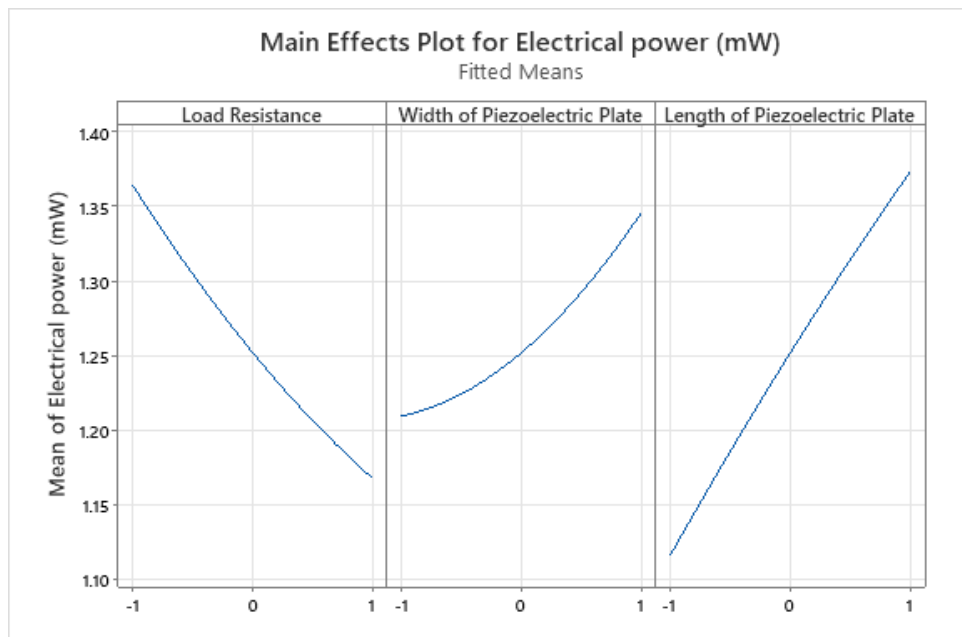


**Figure 15:** Main Effect Plots for Electric power

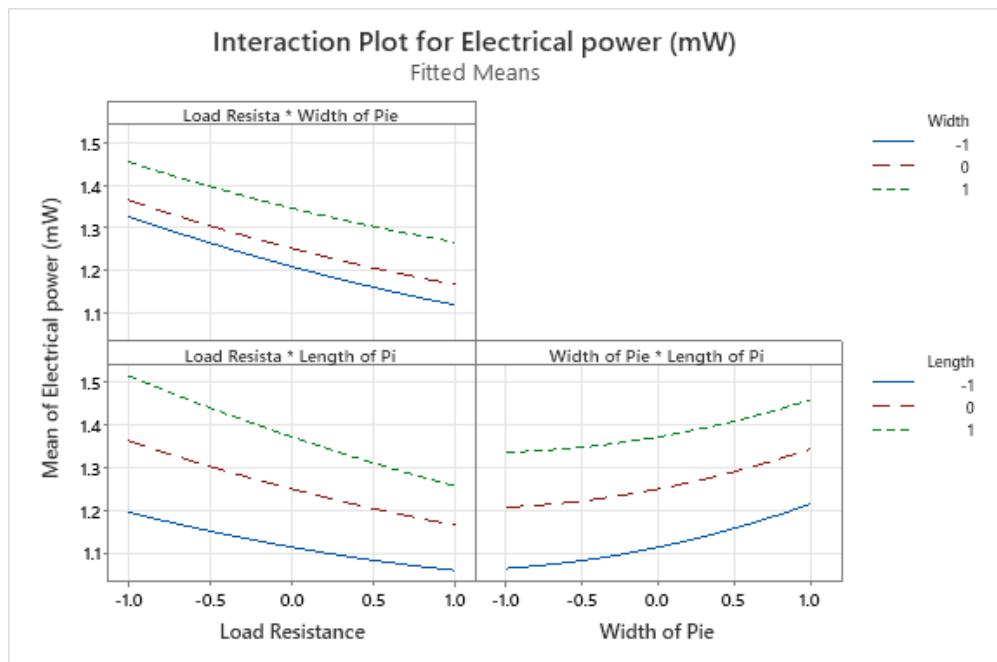


**Figure 16:** Interaction Plots for Electric power

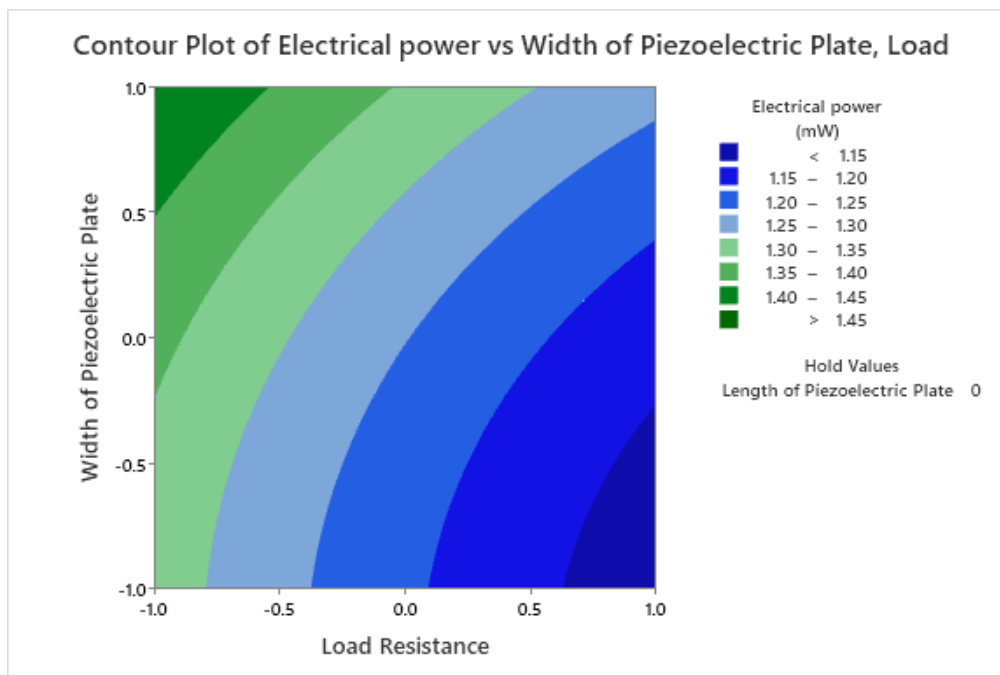


**Figure 17:** Contour Plot of Electric power vs Width and Load

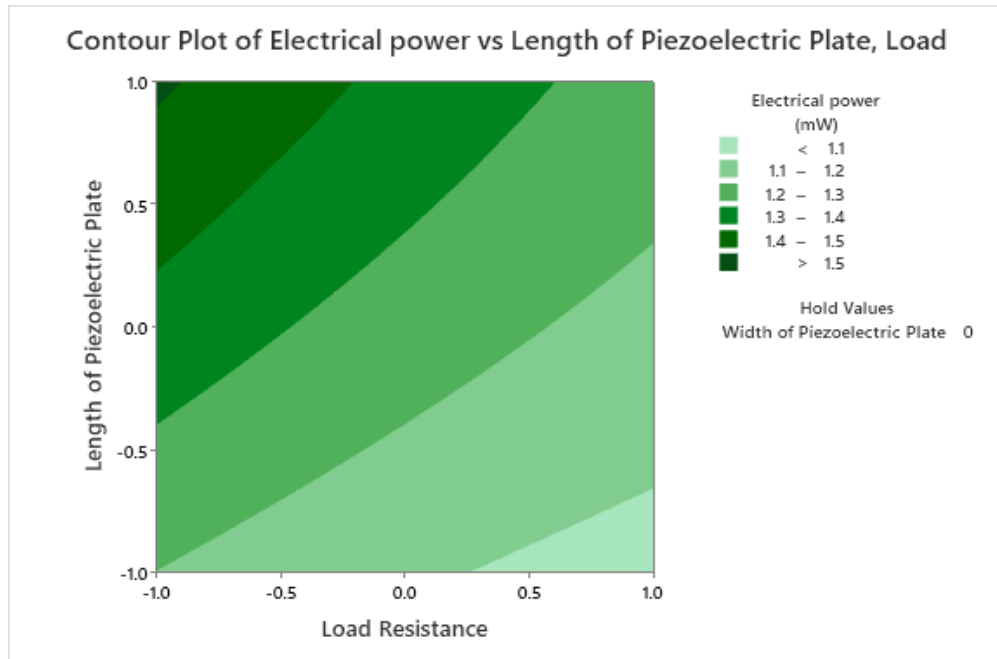


**Figure 18:** Contour Plot of Electric power vs Length and Load

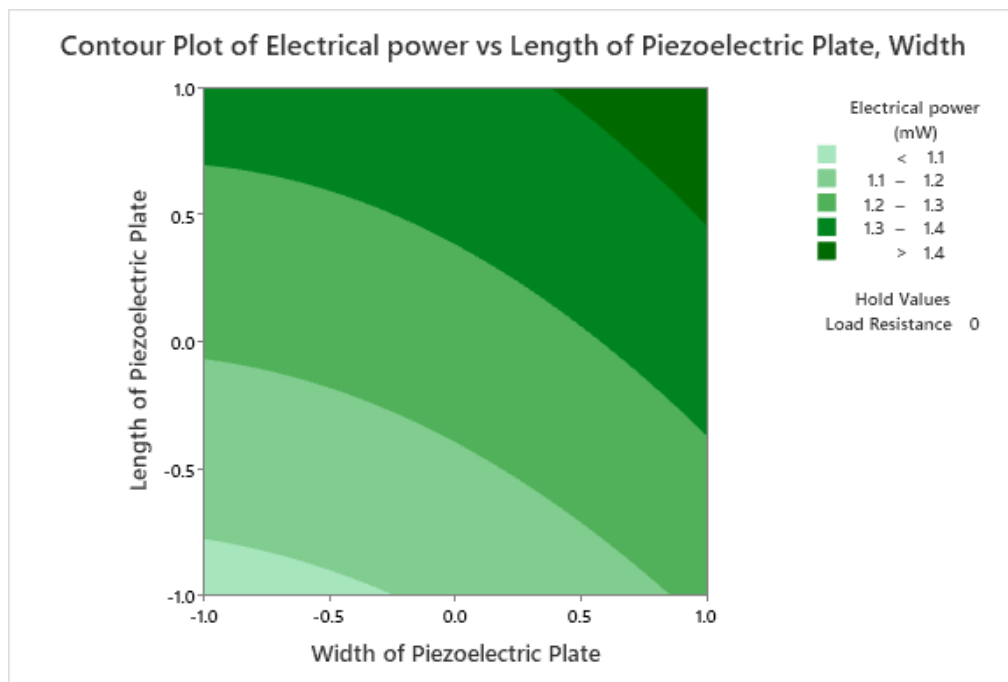


**Figure 19:** Contour Plot of Electric power vs Length and Width

Figure 19 shows the Contour Plot of Electric power vs Length and Width. Table 10 discusses the Fits and Diagnostics for Unusual Observations for voltage. The Contour plots for the electric power vs load and length in Figure 18 show that there is an increase in electric power generated as the load resistance decrease and the length increases. A similar case exists between the width and the load. The main effect plots in Figure 15 further show that all three factors are statistically significant when generating electric power using the

piezoelectric harvester. A direct relationship exists between the electric power, length and width while an inverse relationship exists between the electric power and the load.

### 3.4 Optimisation

This section details the optimisation procedure mentioned earlier in the methodology. The optimisation was determined to maximize electric power and voltage and maintain a constant frequency. To achieve this, the Minitab 18 (2020) software was deployed as a tool. Here, the statistical function in the Domain of Design of Experiments (DOEs) named the response surface methodology was activated for analysis based on the data used for the present study. In particular, the feature on response optimisation was engaged whereby the responses to be optimised are declared in the functional interactive features. The responses of interest are the electric power and voltage. The interaction with the response surface methodological tool in Minitab 18 (2020) provided the opportunity to have access to all three responses of electric power, voltage and resonant frequency. However, the software was activated and instructed to maintain the resonant frequency as a constant response while optimising the two other responses of electric power and voltage without declaring a target value. The outputs of the simulation were optimised as follows: the electric power and voltage were maximized while keeping the frequency constant. The procedure generates the table of responses (Table 13). The goal that Table 13 declares is to maximize the electric power and the voltage. Thus, a lower electric power, according to the previously generated table (i.e. Tables 11 and 12), shows the electric power voltage and resonant frequency based on the different input parameters. Notice that the input parameters are the length, width and the electric load.

Thus, the weight class and importance are shown in the table. The weight class shows the importance of each of the parameters as an attempt is made to optimise them. The target in Table 13 shows the maximum value of the electric power generated and the maximum value of voltage generated on top of previous tables based on the different input parameters of the Box Behnken Design of Experiments. This was previously analyzed using Minitab 18 (2020) to yield various experimental values. These were also introduced into COMSOL Multiphysics software to generate electric power and voltage outputs. Thus, the maximum is the target value in Table 13, which is 1.5239 for electric power and 6.19856 for the maximum voltage. These two values are the target the analysis aims to achieve. Moreover, the lower electric power value is obtainable from the previous table while the lower voltage is the previous table's value.

**Table 13:** Parameters

Response	Goal	Lower	Target	Upper	Weight	Importance
Electrical power (mW)	Maximum	1.05410	1.52397		1	1
Voltage(v)	Maximum	5.13610	6.19856		1	1

Table 14 shows the solution for each of the formulated problems. The solution will yield the maximum length, width and load resistance that can yield what is close to the target value, which is the maximum value. This is displayed in coded coefficients, which implies that 1 represents the maximum value for the input named length. This, according to Table 1 is 23 for the length of the piezoelectric plate. The value of 1 for the width also represents 16, which is the width of the piezoelectric plate. If it had zero, it would have represented 14 for the width. For the length, if it had given a value of zero, it would have represented 22 for the length of the piezoelectric cantilever system. It is done in the coded coefficient where -1 is the lowest value. If it had been given for the width, the researcher would have picked 13. If it had given the researcher - 1 for the length, it would have been 21. However,

in referring to Table 14, the load resistance gives  $-0.474747$  which represents a coded coefficient closer to  $-1$  for the load resistance.

According to Table 1,  $-1$  represents  $11$  for the load resistance. Thus, by interpolation,  $-0.4747$  gives  $12.05$  for the load resistance which is close to  $11$  for the load resistance. Notwithstanding  $-1$  from Table 1, the load resistance means  $11$ . Also,  $-0.4747$  in Table 14 for the solution mean of  $12.05$  for the load resistance. Thus, the values of  $12.05$  for the load resistance and also a value of  $16$  for the width and a value of  $22$  for the length of the piezoelectric plate, are the optimised values that will result in close values to the target values in Table 13. The above discussion is for the solution table. It could also be noted that the voltage fit is shown, and the voltage is obtained. Also shown is the electrical power fit, which shows the optimised value. Also, the optimised value for the voltage is in Table 14. The electrical power is  $1.5222$ , close to the target value of  $1.523$ . For the voltage, the value obtained is  $6.05$ , which is relatively close to  $8.1$  of the target value. Thus, the particular load input values, which are the width of the piezoelectric plate and length of the piezoelectric plate as  $-0.4747$ , which represents  $12.05$  and also the width at the code value of  $1$  and length at the coded value of  $1$  as well, which is the values previously mentioned. It will yield an electrical power output of  $1.5952$  and a voltage fit of  $6.053$  in the solution table. Moreover, it reveals that the fit for the voltage aligns with the target values.

**Table 14: Solution**

Solution	Load Resistance	Width of Piezoelectric Plate	Length of Piezoelectric Plate	Electrical power (mW)Fit	Voltage(v) Fit	Composite Desirability
1	-0.474747	1	1	1.52222	6.05374	0.927626

It could also be observed that from Table 15, which shows the response prediction, the load value, width value and the length value are repeated. Thus, the response being attempted to optimise is the electrical power and voltage. The analysis revealed the fit of these values, which are close to the targeted values in Table 13. The  $S_e$  fit implies the standard error of fits it shows that there is very minimal uncertainty in the prediction.

**Table 15: Multiple Response Prediction**

Variable		Setting			
Load Resistance		$-0.474747$			
Width of Piezoelectric Plate		$1$			
Length of Piezoelectric Plate		$1$			
Response	Fit	SE Fit	95% CI	95% PI	
Electrical power (mW)	$1.5222$	$0.0133$	$(1.4881, 1.5564)$	$(1.4718, 1.5726)$	
Voltage(v)	$6.0537$	$0.0301$	$(5.9764, 6.1311)$	$(5.9396, 6.1679)$	

Thus,  $0.01$  for the electrical power means the error between the target value and the fit value. Also, the  $0.03$  for the voltage implies the error between the target value and the fit value. The  $95\%$  CI indicates the confidence interval for electrical power, which means that the confidence interval for electrical power is between a value of  $1.4881$  and  $1.5364$ . The confidence interval indicates high ( $95\%$ ) confidence that the value will be between those two points, which is  $95\%$  certainty that the value will always fall between the two boundaries. The prediction interval also means that there is  $95\%$  per cent confidence that the value will fall between  $1.4718$  and  $1.57126$ . These two points show the range of individual observations falls during optimisation. Similarly, for the voltage, the confidence interval is between  $5.7964$  and  $6.1311$  and the prediction interval is between  $5.9396$  and  $6.16719$ . By referring to the solution table the electrical power falls between that confidence

interval and also lies between the prediction interval. The voltage fit also falls between that confidence interval given in Table 15. The voltage fit also falls between that prediction interval given in Table 15.

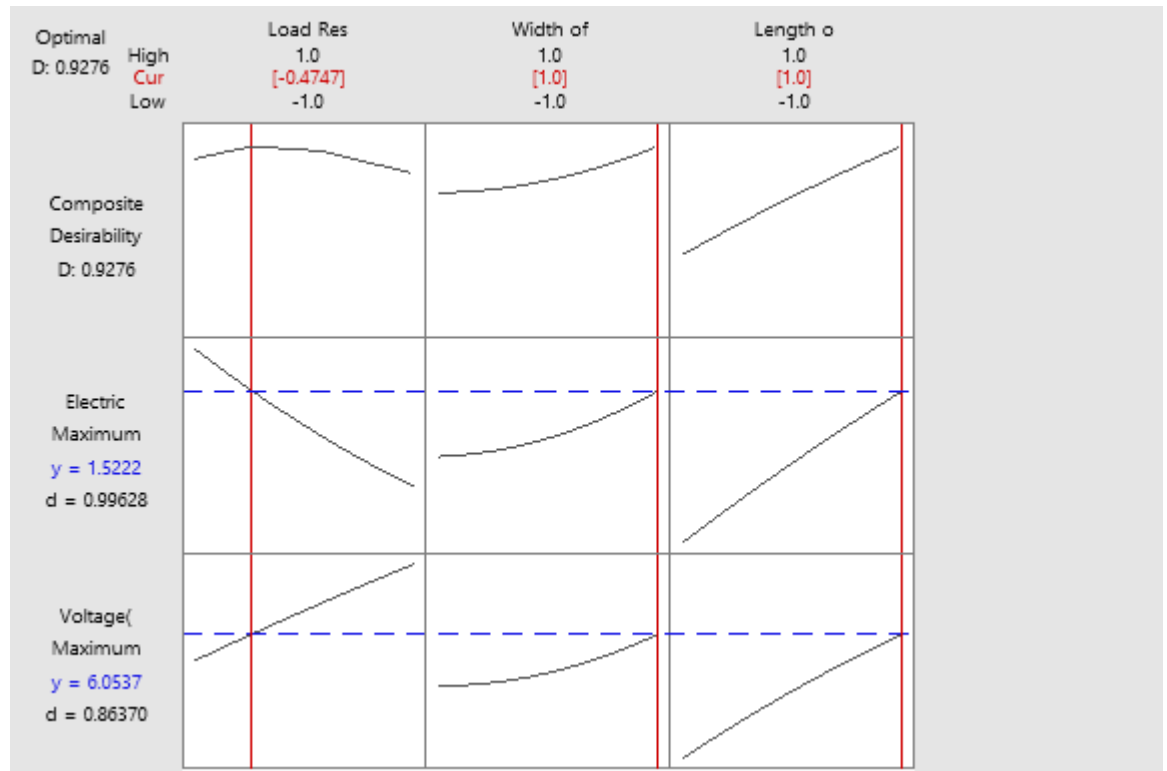


**Figure 20:** Optimisation main effect plot.

Moreover, Figure 20 shows the main effects plots. Here, there is not much difference between them. The maximum electrical power is 1.552. The maximum load output is where the slanted line on the 6<sup>th</sup> block touches the interval line, where the line represents the maximum value. Also, note that the width also touches the line. However, the load resistance across values meets it at a particular point where the negative 0.4747 falls, which represents the coded coefficient of 20.05 for the real value and 0.4747. The same explanation may be given for the voltage. The confidence line could be observed where the length and the width touch the line. The load resistance cuts through that line at -0.4747. Under the width, load and resistance, the researcher observes a value of 1.0 and -1.0, the maximum and minimum values given. Thus, load resistance falls at -0.4747, which is the current value that the calculations fall within. Therefore, these main effects further explain the tables to reveal what those three optimised values are, which are the electrical power, and voltage while hearing the frequency constant.

### 3.5 Comparison of BBD with the Taguchi method

The Box Behnken design method here imposes a 3 by 3 design, which means 3 factors and 3 levels while the Taguchi method imposes a 3 x 4 design which means a 3-factor and 4-level design was used as shown in Table 16.

**Table 16:** Comparison of Box Behnken Design and Taguchi Method

S/N	Parameters	Box Behnken Design	Taguchi Method
1	Electric Power	1.52MW	1.78MW
2	Voltage	6.05V	5.97V
3	Frequency	65Hz	65Hz
4	Optimised Length	23mm	23mm
5	Optimised Width	16mm	17mm
6	Optimised Load Resistance	12.05	10
7	Number of Experiment	15	16
8	Advantage	Better Precision and well-detailed	Simple and Quicker
9	Limitations	Computationally Intensive and requires statistical experience	Limited in handling higher-order interactions and overlooks the complex relationship

The Box Behnken design utilizes a precise optimisation by analyzing the quadratic relationship between the parameters and response i.e. how the response values here are modelled as functions of the input parameters with the ANOVA tables given above. Although the Taguchi method used by Ismail and Husaini (2021) achieves a slightly higher electric power output it lacks the precision in analyzing the parameters interactions seen in the Box Behnken method. Hence the BBD method gives a more robust analysis, interaction between parameters input and output and better precision with its thorough analysis. From both experiments, it is observed that even though all parameters are significant, the Length is more significant as shown on the ANOVA and coded coefficient tables. Hence the variations of length are seen to have the greatest impact on the output values, this implies that the length has a substantial effect on all the output parameters as small changes in length yield a massive change in the output parameters.

For a design engineer, this entire analysis provides a roadmap to create an optimised piezoelectric cantilever energy harvester. The major focus should be on the length as a primary design parameter while tuning the other parameters to fit the design requirement. Furthermore, the results obtained in the present study, using the Box Behnken Design, were compared with those presented by Ismail and Hussein (2021) to establish their differences and similarities. The comparison results are shown in Table 16. Here, the various values of the parameters are shown including the voltage generated, frequency obtained and electric power. Then the optimised length, width and load resistance are shown. All these are given under varying experimental counts. The Box Behnken Design method uses statistical analysis. The Taguchi method uses the same number of factors as the Box Behnken Design to conduct analysis.

Here, the same three factors are used in both Box Behnken Design and Taguchi methods. The Box Behnken Design uses three levels while the Taguchi method uses four. The Taguchi method uses an orthogonal array of L16 for 16 experiments while the Box Behnken Design method performs its analysis in 15 experiments. The optimal load for the Box Behnken Design method is 12.5 while that of the Taguchi method is 10. The optimised width for the Box Behnken Design method is 16 while for the Taguchi method, it is 17. The optimised length for both methods is 223. The frequencies are the same in both methods. However, the voltage obtained through the Box Behnken Design method is higher than the obtained value through the Taguchi method by a small amount. For electric power, the Box Behnken Design method gives a lower value than what was obtained using the Taguchi method.

Notwithstanding, one of the advantages of the Box Behnken Design method is that it is a more precise optimisation method than the Taguchi method. The Box Behnken

Design method is suitable for systems requiring detailed parametric investigations. It could be seen from the experiments conducted using the Box Behnken Design method that between the input and output data, there is correspondence with each other. This observation is valid from the previous graphs plotted in the results section of this article, including the ANOVA table. Furthermore, the Taguchi method is simpler and quicker than the Box Behnken Design method. The Taguchi method is useful in the initial screening of parameters to understand what parameters are important. However, the Box Behnken Design method goes into detail about the parameters.

Notwithstanding, one of the limitations of the Box Behnken Design method is that it is computationally intensive, requiring huge computational power and statistical experience. However, the Taguchi method is limited in handling higher-order interactions. Thus, when there exists a high interaction among the factors parameters of a system the Taguchi method cannot function properly. It overlooks the complex relations that the Box Behnken Design can gain insight into. Now, the most important parameter in the process is length. It can be observed in all the experiments that length is one of the key factors. The reason is that a cantilever structure is the object of analysis and the higher the length, the more the vibration intensity.

Also, higher length implies more structural details to be accounted for in the cantilever system. So, what should the design engineer do with the outcome, and why the following could be mentioned? The design engineer can account for the length of the piezoelectric cantilever as the primary determining factor. It tries to balance the other factors like the load resistance and the width. Thus, the design engineer should prioritize length, which should be the primary focus for the design and the choice of parameters. The length determines things like the resonant frequency, the voltage and the power output. Thus, fractioning this length parameter can yield a substantial improvement in the energy harvesting system. The design can be tailored to the application needed. The design can be aligned with the vibration frequency of the targeted environment. It can be seen that the optimised frequency is 65Hz. So, the targeted environment should be about this value of 65. This is a low-frequency system. The other parameters that may be considered apart from the length are the load resistance and width. These are secondary factors while length is the primary factor. Notice that land affects the electrical power and other parameters such as the width influences the mechanical stability of the cantilever system and the voltage given out by the system. With the information given above, additional tests on the runs with COMSOL metaphysics software can be conducted to observe the outputs before conducting the fabrication of the system in real terms.

### **3.6 Implications of the study**

This study offers valuable insights into the parameters and responses of a cantilever-based piezoelectric energy harvesting system with experimental details taken from the designed model by Ismail and Husaini (2021). Using the COMSOL software, the authors provided evidence on the bi-aspect bi-morph cantilever with had zirconate titanate and structural steel materials for the top and bottom layers of the piezoelectric structure as well as the middle parts of the substrate, respectively. A comparative analysis was made of the Box Behnken Design method with the literature results of the Taguchi method. Such an effort intends to enhance the clarity of the contribution highlighted in this work. Earlier, a literature review was conducted on the topic so that the contribution of this study would become clear by exposing research gaps. From the application of the Box Behnken Design methodology to the data used in this work, the results show that the parameters were effectively optimised. This was done by establishing the optimal set of variable levels that may run with fewer experiments; thus is an advantage over the full factorial design method that could have been applied in the alternative. Thus, the BBD method significantly

contributes to the energy harvesting literature by installing benefits of superior resource use, cost reduction and increased efficiency in the energy harvesting system studied.

More importantly, the comparative results of the BBD method with the Taguchi method strengthen the contribution of this work, placing the BBD method as a robust yet competitive method to conserve energy harvesting resources. However, effective management skills are essential for BBD's methodical implementations in the energy harvesting system. In general, it implies that despite having the results of the BBD method, failure to put the right personnel in place to implement the results could bring negative influences on the outcomes of the system and thus shrink the opportunity of the system to conserve resources. This study contributes theoretically and practically to engineering practice, which permits energy systems to secure substantial and crucial resource conservation and project them in advantages to remain competitive in the industry. It is expected that by adopting this robust structure energy harvesting systems could enjoy more stability and be sustainable since their resources are always being conserved. Moreover, the engineering manager of the energy harvesting system is in control of the risks to which the operators of the system are exposed. The engineering manager acts well by implementing the optimisation results of the BBD method in the system, allowing the reduction of risks which are constant threats to the safety and stability of the system.

#### 4. CONCLUSION

This study used the Box Behnken Design Method to demonstrate the optimisation potentials of the parameters of the energy harvesters using the piezoelectric cantilever materials. The study accounts for the quadratic model attributes and the building of the sequential designs of the problem. Future studies may be on integrating multicriteria methods with the Box Behnken design methods for a more robust analysis of results. Moreover, this work considered three parameters, namely, load resistance, the width of the piezo plate and the length of the piezo plate. Meanwhile, the optimal values of these parameters are as follows: 12.05, 16mm and 23mm respectively. Furthermore, this is the first time that the Box Behnken design will be used to conduct optimisation decisions for the piezoelectric cantilever-based energy harvesting system.

#### ACKNOWLEDGEMENT

Thanks to all that contributed to the success of this work

#### REFERENCES

- [1] Chesnes J.J., Nelson D.A., Kolodziej J.R. 2024. Optimisation of Vibration-Based Reciprocating Compressor Valve Health Classification. *IFAC-PapersOnLine*. 58(28):294-299. <https://doi.org/10.1016/j.ifacol.2025.01.010>
- [2] Gong S., Lu H., Zeng Z., Wang Z., Li D. 2019. Vibration Suppression of Rotating Arm in LED Chip Sorter Using Feedforward-Feedback Control with an Optimal Curve. *Precision Engineering*. 56:513-523. <https://doi.org/10.1016/j.precisioneng.2019.02.009>
- [3] Zhao N., Zhang J., Ma W., Jiang Z., Mao Z. 2022. Variational Time-Domain Decomposition of Reciprocating Machine Multi-Impact Vibration Signals. *Mechanical Systems and Signal Processing*. 172, Article 108977. <https://doi.org/10.1016/j.ymssp.2022.108977>
- [4] Guan H., Ma H., Chen X., Mu Q., Zeng Y., Chen Y., Wen B., Guo X. 2025. Nonlinear Vibration of Rotor-Bearing System Considering Base-Motion and Bearing-Misalignment. *Mechanism and Machine Theory*. 206, Article 105933. <https://doi.org/10.1016/j.mechmachtheory.2025.105933>
- [5] Wu K., Liu Z., Ding Q. 2020. Vibration Responses of Rotating Elastic Coupling with Dynamic Spatial Misalignment. *Mechanism and Machine Theory*. 151, Article 103916. <https://doi.org/10.1016/j.mechmachtheory.2020.103916>

- [6] Wang D., Chen L., Long Y., Bao R., Sun Y. 2025. HLSM-MIPV Algorithm of Unbalance Vibration Suppression of Dual-Rotor in Contra-Rotating Propfan. *Journal of Sound and Vibration*. 595, Article 118761. <https://doi.org/10.1016/j.jsv.2024.118761>
- [7] Yu P., Hou L., Jiang K., Jiang Z., Tao X. 2024. Dynamic Modeling and Nonlinear Analysis for Lateral-Torsional Coupling Vibration in an Unbalanced Rotor System. *Applied Mathematical Modelling*. 126: 439-456. <https://doi.org/10.1016/j.apm.2023.11.005>
- [8] Ran L., Halim D., Thein C.K., Galea M. 2024. Lateral Vibration Attenuation of a Rotor System Using an Axial Control Mechanism with Resonance Detuning. *Mechanical Systems and Signal Processing*. 211, Article 111220. <https://doi.org/10.1016/j.ymsp.2024.111220>
- [9] Tang J., Li C., Zhou J., Wei W., Wu Z. 2025. Vibration Suppression Control and Anti-Eccentric Load Correction Mechanism of Magnetic Levitation Decoupling Platform. *Mechanical Systems and Signal Processing*. 225, Article 112314. <https://doi.org/10.1016/j.ymsp.2025.112314>
- [10] Liu C., Shi M., Zhang W. 2025. Comparative Study of Six Generic Models for Dual-Objective Vibration Mitigation and Energy Harvesting. *Engineering Structures*. 327, Article 119640. <https://doi.org/10.1016/j.engstruct.2025.119640>
- [11] Li P., Gao L., Wang Y., Liu Z., Zhu L., Su T., Huang Y., Wang Y. 2025. Experimental Study on Vortex-Induced Vibration of Risers Fitted with Detached Splitter Plate Vibration Suppression and Energy Harvesting Device. *Ocean Engineering*. 320, Article 120318. <https://doi.org/10.1016/j.oceaneng.2025.120318>
- [12] Le, V. D. 2024. Finite Element Analysis and Optimisation of the Piezoelectric Circular Diaphragm Energy Harvester. *Applied Mechanics and Materials*. 922(1):111-121. <https://doi.org/10.4028/p-mbogv9>
- [13] Liao, H., Wu, T., Gao, G., Wu, X., and Gao, F. (2024). Shape optimisation of a non-uniform piezoelectric bending beam for human knee energy harvester. *Smart Materials and Structures (Print)*. <https://doi.org/10.1088/1361-665x/ad78ce>
- [14] Alzuwayer, B., Almokmesh, S. F., Alhashem, A., and Alotaibi, T. (2024). Multi-Variable Optimisation to Enhance the Performance of a Cantilevered Piezoelectric Harvester. *Energies*. <https://doi.org/10.3390/en17174274>
- [15] Xu, Y., Xian, T., Chen, C., Wang, G., Wang, M., and Shi, W. (2024). Mathematical Modeling and parameter optimisation of a stacked piezoelectric energy harvester based on water pressure pulsation. *Energy*. <https://doi.org/10.1016/j.energy.2024.130530>
- [16] Zheng, X., He, L., Wang, S., Liu, X., Liu, R., and Cheng, G. (2023). A Review of piezoelectric energy harvesters for harvesting wind energy. *Sensors and Actuators A: Physical*. <https://doi.org/10.1016/j.sna.2023.114190>
- [17] Parvathi, S., Raju, S., Srikanth, M., and Kusuma, Y. G. (2023). Design, Simulation, Optimisation and Performance of a MEMS-Based Piezoelectric Energy Harvester. 2023 2nd International Conference for Innovation in Technology (INOCON). <https://doi.org/10.1109/inocon57975.2023.10101260>
- [18] Aceti, P., Rosso, M., Ardito, R., Pienazza, N., Nastro, A., Baù, M., Ferrari, M., Rouvala, M., Ferrari, V., and Corigliano, A. (2023). Optimisation of an Impact-Based Frequency Up-Converted Piezoelectric Vibration Energy Harvester for Wearable Devices. *Italian National Conference on Sensors*. <https://doi.org/10.3390/s23031391>
- [19] Hu, S., Fitzer, U., Stindt, S., and Bechtold, T. (2022). Topology Optimisation of a Folded Beam Piezoelectric Energy Harvester. *IFAC-PapersOnLine*. <https://doi.org/10.1016/j.ifacol.2022.09.124>
- [20] Li, H., Liu, K., Deng, J., and Li, B. (2023). Validation and optimisation of two models for the magnetic restoring forces using a multi-stable piezoelectric energy harvester. *Journal of Intelligent Materials Systems and Structures*. <https://doi.org/10.1177/1045389x221151064>
- [21] Liao, H., Wang, Y., Shi, Q., Huang, R., and Gao, F. (2023). Optimisation of a Piezoelectric Bending Beam-based Human Knee Energy Harvester. 2023 IEEE International Conference on Mechatronics and Automation (ICMA). <https://doi.org/10.1109/icma57826.2023.10215790>
- [22] Ismail, M. H. Bin, and Husaini, Y. (2021). Design and Optimisation of Piezoelectric Cantilever for Energy Harvesting Application by Using Taguchi Method. *International Journal of Academic Research in Business and Social Sciences*, 11(9). <https://doi.org/10.6007/ijarbss/v11-i9/10342>
- [23] Abdullahi Y.U., Oke S.A. (2022). Optimising the Boring Parameters on CNC Machine using IS 2062 E250 Steel Plates: Taguchi-Pareto-Box Behnken Design and Taguchi-ABC-Box Behnken Design Perspectives, *Engineering Access*, 8(2): 219-241.
- [24] Abdullahi Y.U. and Oke S.A. (2022), Optimisation and Selection Of Boring Process Parameters for IS 2062 E250 Steel Plates Using Hybrid Taguchi-Pareto Box Behnken-Genetic Algorithm Method, *Indonesian Journal of Industrial Engineering & Management*, 3(2):131-150. <https://doi.org/10.22441/ijiem.v3i2.15443>
- [25] Nwafor S.C., Oke S.A., Ayanladun C.A., (2020), Optimisation of Casting Geometries for A356 Alloy Composites Reinforced With Organic Materials Using Box-Behnken Design Methodology, *Journal of Applied Science & Process Engineering*, 7(2): 524-553.
- [26] Abdullahi Y.U. and Oke S.A. (2022), Optimising the Machining Process of IS 2062 E250 Steel Plates With The Boring Operation Using A Hybrid Taguchi-Pareto Box Behnken-Teaching Learning-Based Algorithm, *International Journal of Industrial Engineering and Engineering Management*, 4(2):49-63.
- [27] Abdullahi Y.U., Oke S.A., Rajan J., Jose S., Adedeji W.O. (2024), Coupled Taguchi-Pareto-Box Behnken Design-Grey Wolf Optimisation Methods for Optimisation Decisions when Boring IS 2062 E250 Steel Plates on CNC Machine, *Engineering Access*, 10(1): 28-41.